EXPERIMENTAL AND ANALYSIS OF THE EFFECTIVENESS OF FILM COOLING IN GAS TURBINE BLADE TECHNIQUE

Hyder H. Balla
Al-Furat Al-awsat Technical University, Engineering Technical Collage Najaf, Iraq
Received on 18 December 2016 Accepted on 22 January 2017

Abstract

This study employed the use of experimental data of film cooling effectiveness using corrugation film cooling hole. Effects of blowing ratio in conjunction with twisted angles (0°, 90°, 180°, 270° and 360°) were also investigated. Recently, the utilization a vortices in enhancing thermal transfers is becoming increasingly attractive as a result of its dual advantages including its surfaces that are extended, turbulent twisted holes as well as coarseness. Results of enhancement in the effectiveness ranging from 1.2–2.2 times those from conventional smooth film cooling holes with significantly increased coefficient of thermal transfer ranging from 1.50 to 2.70 times those of the conventional film cooling holes with smooth surfaces. Both the numerical and the experimental analysis of the effectiveness of film cooling were authenticated by results from pervious related studies. The authors found and concluded thus, effectiveness of twisted film cooling holes at rectangular spiral corrugation shape was higher in comparison to holes with cylindrical shape. The effectiveness of film cooling for the twisted holes were observed to be hugely influenced by inclination angle between the main and the secondary holes of the film cooling hole antivortex.

Key words: film cooling, anti-kidney vortex, geometry of jet, experimental work, cooling performance, losses

التحديد التجريبي لفعالية تقنية التبريد الغشائي لريشة التوربين الغازي

مدرس دكتور/ حيدر حسن عبد بالة

الكلية التقنية الهندسية- نجف/ جامعة الفرات الاوسط التقنية

الكلمات المفتاحية: تبريد غشائي، مضادات الدوامات ، هندسة النفاثات ، عمل تجريبي، كفاءة التبريد، خسائر

1. Introduction

Recently, the frequency of utilizing film cooling in the reduction of the heat burden on high-pressure turbine airfoil in attempt to achieve higher turbine inlet temperature for the purpose of enhancing thermal efficiency is on the increase. The heat transfer enhancement basically based on the adopting of many tools that induces a swirl and vortices at the secondary flow region, which mixed the fluid layers with the core flow and increasing the surface area [1]. A film of cooling air is then produced over the blade surface, thereby reducing the overall heat burden ~~to~~ on the blade surface. The effect of swirling movement on film cooling has equally been demonstrated to be important in both turbine blades and turbine vanes [2]. This is owing to the fact that in recent air-cooled turbine blade and turbine vanes , impingement cooling and a serpentine flow passage with a turbulent promoter are employed in cooling the airfoil and end wall internally. The thrust for an improvement in cooling performance has made film cooling designs the focus of several studies.

With regard to this, one of the main aspect of approach in achieving enhanced cooling performance has been shown to be the alteration of the morphology of film cooling hole to modulate jet lift off and subsequently reduce the overall burden of hot gas entrainment which is typically associated with the conventional round jets. Even though single film cooling hole designs usually involve range of geometrical variables such as the shape of the hole, jet inclination angle (β) and twisted film cooling hole angle (α), only variations of the hole configuration was considered in the present work. Detailed reports on other geometric measurement has been previously documented in related studies by other authors [3]. James D. [4] investigated "anti-vortex" film cooling concept and proposed the addition of two additional holes from the primary holes for the purpose of generating vortices to counter the detrimental kidney vortices from the major jet as depicted in Fig. 1. The concept of anti-vortex film cooling hole had been computationally modelled for single rows of 30° angled holes on a flat surface. A little modification in the concept of the anti-vortex whereby the branched holes exit adjacent to the major hole has been computationally investigated for blowing ratios of 1.0 and 2.0 at density ratios between 1.0 and 2.0. The outcome of the computational investigation show that the modified design improves the effectiveness of the film cooling relative to the round hole baseline and previous anti-vortex cases, which confirms the findings of the experimental studies.

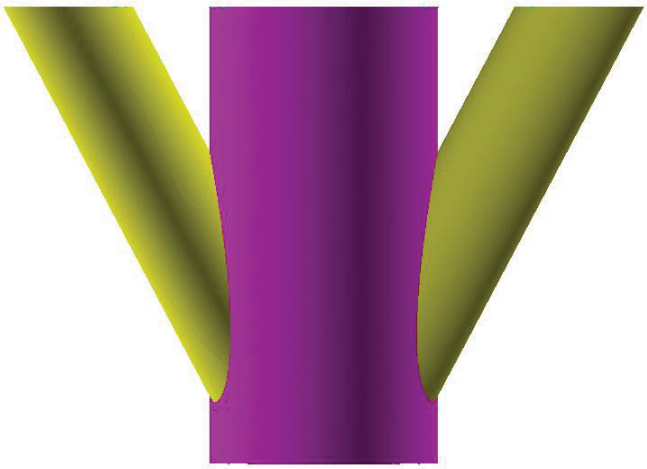

Fig. 1 Front view of the adjacent anti-vortex design [4].

A commonly known and exhaustively investigated property of the flow from round film cooling holes ~~is~~ has been shown to be the counter rotating vortex pair which is responsible for the separation of the cooling jet from the surface at a significantly high blowing ratio. This phenomenon is depicted in Fig. 2. The counter-rotating vortex pair entrains the hot free stream gas and lifts the coolant away from the surface، thereby significantly reducing its efficiency. The counter-rotating vortex pair ~~is~~ has been previously described by Haven et al. [5]

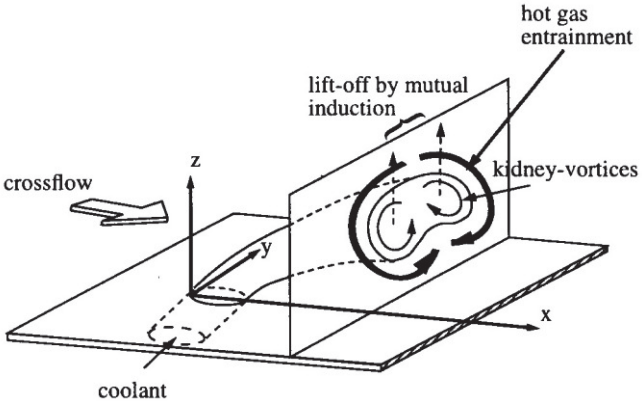

Fig. 2 Counter-rotating vortex pair and jet lift-off, [5]

Several investigations on film cooling effects have been conducted. Early works in this area had been summarized in a previous review [6] while the latest in this field were reviewed by Bogard and Thole [7]. Other researchers [8, 9] have similarly investigated the flows blowing via inclined discrete holes. Several other experimental endeavors to enhance film cooling effectiveness through adoption of film cooling holes whose exits are expanded had been conducted by several other authors [10-13]. An excellent and summarized profile of film cooling effects has been recently documented [14]. Several other new ideas for regulating an anti-kidney vortex structure had been similarly documented. Two other different film cooling designs with different compound angles had been previously evaluated in a related study [15]. Recently, additional cooling air jet has been proposed in a circular film cooling hole to modulate and subsequently crash the kidney-type vortex [16]. A generator of the delta vortex origin was placed at the downstream of the ejection hole. Amazingly, the vortex generator introduced was observed to be very effective in ~~producing~~ generating an anti-kidney vortex pair [1]. Abdulwahid et.al. [17] had experimentally investigated heat transfer dynamics within corrugation film cooling holes of varying cross sectional area square, rectangular and circular. Circumstances of this investigation of blowing ratios ranging from 0.5-2.0 and hole angle at 30°. The results of experimental studies employing swirling film cooling flow has shown that rectangular film cooling holes induce decrease in the effectiveness of the film cooling at a low swirl but enhanced it at a high swirl number. The resulted anti-kidney vortex pair generated in the said study triggered coolant to be blown toward the wall while concurrently spreading it out along it. A 'sister hole' design which led to an increase in film cooling effectiveness owing to previously established vortex structure which was investigated in an earlier study [18]. Such cooling methods employ the motion of vortex of the cooling air to enhance the coefficient of heat transfer. Additionally, the film cooling air was normally ejected from the air sources, which still maintained either weak or strong vortex. The motion of the vortex in the bleeding film cooling air may enhance the effectiveness of film cooling, especially where the strength of the vortices could blend with the film cooling conditions [19]. In addition to the use of motions of the vortex in the inner cooling airflow. The development of a new cooling method that could make use of actively produced vortex motion in the cooling flow of the film will be very crucial in enhancing the effectiveness of film cooling in an elevated temperature gas turbine for both its vanes and blades. A measurement system that would enable the achieving of the rapid and averaged time mixing of flow fields of the film cooling air and mainstream utilizing laser-induced fluorescence (LIF) technique which was recently developed [20]. It was further demonstrated that the technique could be a powerful tool for studying the mechanisms of the mixing process in film cooling in view of rapid fields. Abdulwahid et. al. [21] investigated a new numerical method of film cooling employing swirling coolant flow via a rectangular twisted film cooling holes with spiral corrugated tube. The constraints of this study were the blowing ratios which ranged from 0.25-4.0 and the angle of hole which was at 30°. The results of the effectiveness of the cooling obtained were compared against a standard untwisted tube. The results of the study revealed that the overall thermal effectiveness was enhanced significantly when the difference in temperature between the air flows was at 25 degrees.

Such enhancement was ~~is~~ supported by heat transfer improvement that was obtained from 19.7% to 57.4%. The influence of swirled film cooling air on the effectiveness of film cooling, employing a twisted tape in a circular cooling hole has been previously investigated and an enhancement in the effectiveness of film cooling in conjunction with the swirling coolant flow was observed [22]. However, the study neither provided quantitative description nor do they present experimental findings that shed more light on the mechanism of film cooling with the swirling flow. Although effects film cooling have been extensively studied, studies treating effectiveness of film cooling with a swirling flow are very few.

Recently, film cooling arrangement aimed at cooling the end wall of first vane of a high-temperature industrial gas turbine built with a hexagonal shell structure with two other inclined impingement nozzles on the cover plate of the hexagonal shell has been proposed. The swirling

coolant flow produced by these inclined impingement nozzles was anticipated to blow through a film-cooling hole on the end wall. This concept could control not only the film-cooling airflow rate but also blowing ratio which could eventually give rise to optimize the effectiveness of film cooling on the end wall. Hence, the current study presents an experimental as well as numerical studies of a new film cooling corrugation shapes (rectangular, circular and hexagonal) in film cooling corrugated holes in order to investigate evaluate the effects of the corrugation shape on effectiveness enhancement and heat transfer coefficient as well as to correlate an empirical expression for effectiveness and heat transfer coefficient.

2. Experimental apparatus and procedure

Table 1 Details of the experimental conditions

			Actual		
Test Model	Re_D	Br	Re_D	Br	T_∞ (°K)
One Hole	6200	0.5	6195	0.52	350
One Hole		1.0	6185	1.0	352
One Hole		2.0	6194	2.01	349
Two Holes		0.5	6201	0.51	350
Two Holes		1.0	6201	1.0	353
Two Holes		2.0	6204	2.0	352
Three Holes		0.5	6210	0.5	355
Three Holes		1.0	6211	1.01	348
Three Holes		2.0	6217	1.98	350.9

The studied configuration:

Three study models are used in this experiment and these were namely Test Models with one hole, two holes and three holes respectively. The 3 different test models were all used in the thermal studies. Figure 3 revealed the well-known non-dimensional configuration of the hole for thermal investigations. The cooling hole employed was a conventional rectangular twisted hole with inclination to the main direction of flow at angle, $\beta = 30^{\circ}$, 45 and 90 as depicted in Fig. 7. The cooling hole was separated in lateral direction at 6D. The diameters of the hole for the thermal and aerodynamics investigation were adjusted to 7 mm while the width and the breath of the plate tested was fashioned to offer the hole length to diameter ratio, l/D = 6. The models tested were produced from acrylic plate and the production precision of ±0.1 mm. The setup of the experiment for the thermal evaluation employed in the current investigation is depicted in Fig. 4. The facility comprises of a wind tunnel utilised for delivering the mainstream air through separate blowers for the secondary air. The test canal cross section was designed to have 150 mm width as well as 150 mm height with a sharp upstream edge to restructure the boundary layer within the test section. The test or study models originated from acrylic plates possessing thermal (heat) conductivity of 0.19 W.m-1K-1 with 7 mm diameter of cooling hole. Thermocouple was placed on the test model to generate data on temperature which are essential for calibration, and were utilised to approximate the emissivity of the test surface. During the determination, the secondary air was regulated at a temperature of 50°K less than the major stream temperature. The IR camera used was FLUKE I400 which has a maximum recording capacity of 30 frames per second with the determination lasting for a period of three minutes. The camera was operated in a long-wavelength infrared band with spectrum ranging from 8 to 13 μm.

Fig. 3. The setup of the thermal experiment.

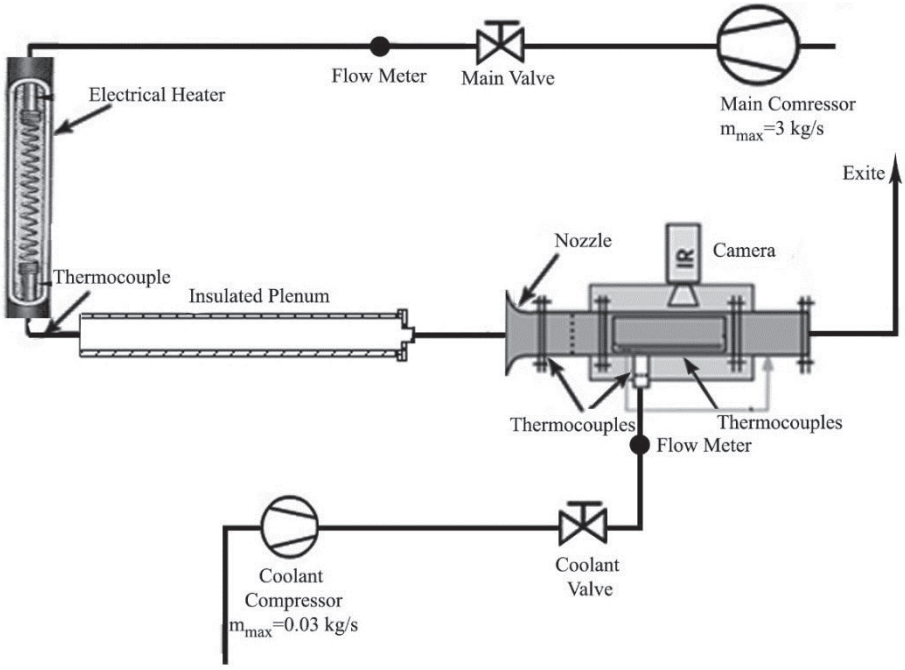

Fig. 4. Experimental set-up scheme.

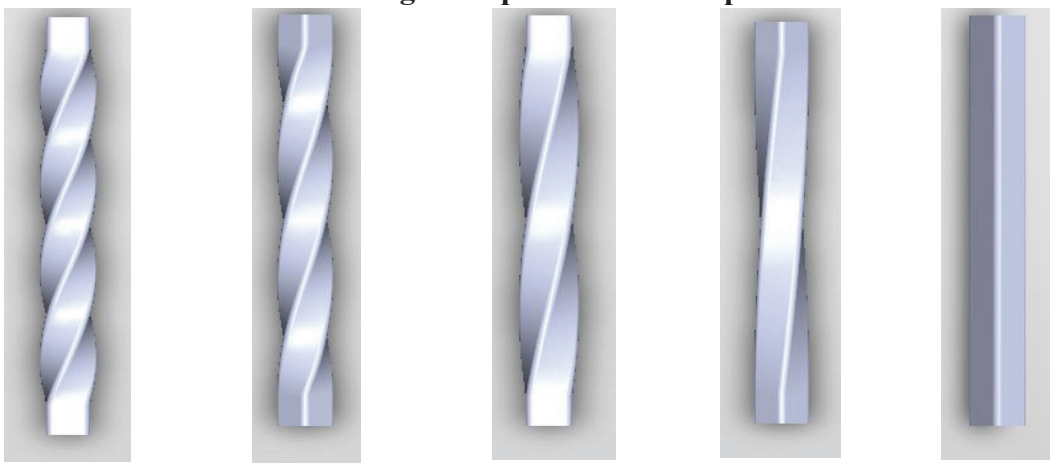

Case 1 (α =360°) Case 2 (α =270°) Case 3 (α =180°) Case 4 (α =90°) Case 5 (α =0°)

Fig.5. Rectangular geometry varied corrugations.

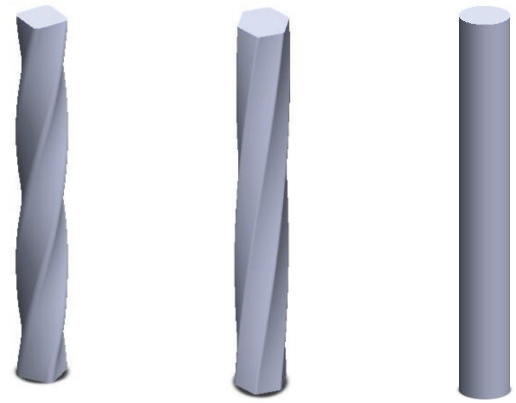

(a) (b) (c)

Fig. 6. Three shapes of corrugation; (a) rectangular (b) hexagonal (c) circular.

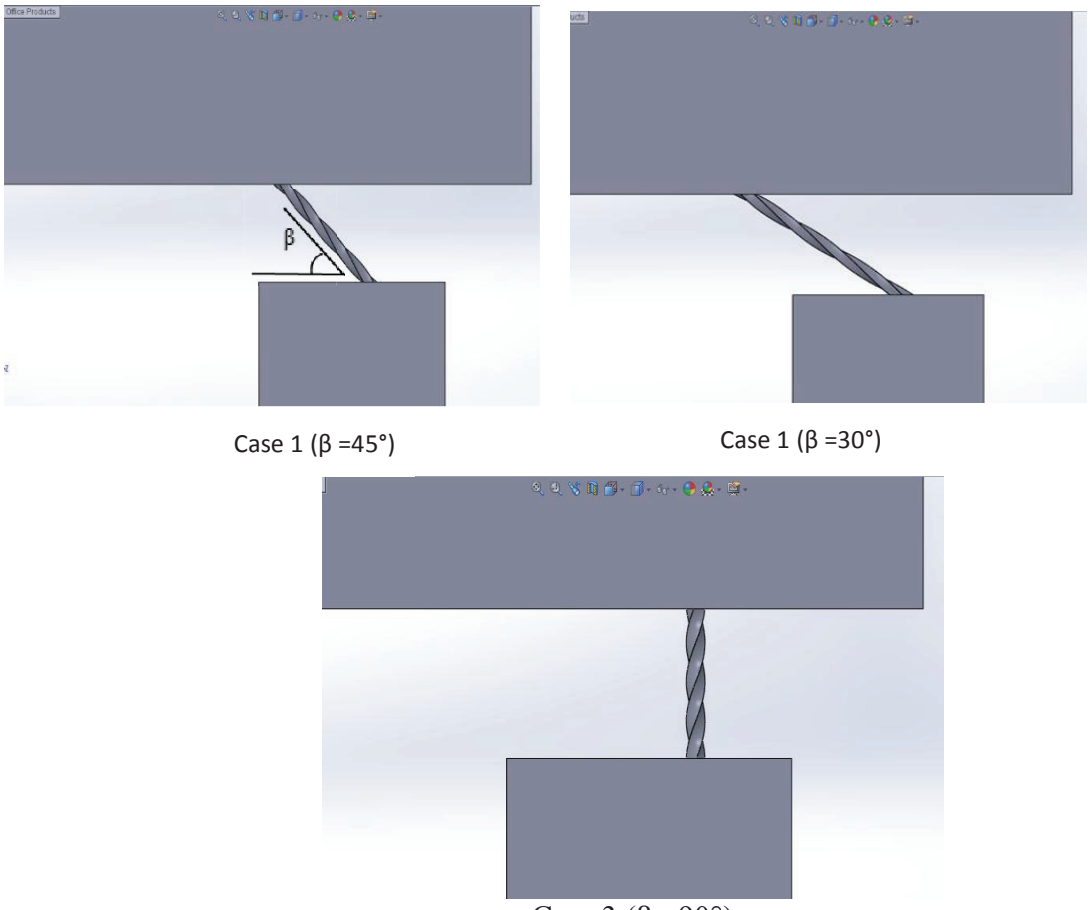

Case 1 (β =45°) Case 1 (β =30°)

Case 3 (β =90°)

Fig.7. Variation of holed angle at 30°, 45° and 90° for rectangular geometry.

Table 2: Film cooling hole of experimental and numerical tests

No. of Hole	Br	β	Re_m	Re_j	Status
1	0.25- 4.0	30°,45° and 60°	$27.56*10^3$	6200	Numerical and Experimental
1	0.25- 4.0	30°,45° and 60°	$30.66*10^3$	6200	Numerical and Experimental
1	0.25- 4.0	30°,45° and 60°	$44.15*10^4$	6200	Numerical and Experimental
1	1.0	30°	$27.56*10^3$	6200	Smooth Hole

					Numerical and Experimental Incropera et. al. [23]
1	1.0	35°	$35.86*10^4$		Smooth Hole Num. Leedom et. al. [25]
2	0.25- 4.0	30°,45° and 60°	$27.56*10^3$	6200	Numerical and Experimental
2	0.25- 4.0	30°,45° and 60°	$30.66*10^3$	6200	Numerical and Experimental
2	0.25- 4.0	30°,45° and 60°	$44.15*10^4$	6200	Numerical and Experimental
3	0.25- 4.0	30°,45° and 60°	$27.56*10^3$	6200	Numerical and Experimental
3	0.25- 4.0	30°,45° and 60°	$30.66*10^3$	6200	Numerical and Experimental
3	0.25- 4.0	30°,45° and 60°	$44.15*10^4$	6200	Numerical and Experimental

3. Numerical procedure

3.1. Geometrical configuration

Stainless steel film cooling holes of spiral corrugation having 7 mm hydraulic diameter were modelled with the same corrugation features and corrugation profile as those of the spiral corrugation film cooling holes used in the experimental tests to curtail the deviation between Experimental and numerical data. In addition, one smooth and one corrugated tubes were also modelled to be numerically simulated as shown in Table 2. Further enhancement were achieved by using corrugation in the turbulent flow region accompanied with pressure drop. Individually corrugated tubes were modelled according to the methods described by Incropera [23] for the purpose of validation.

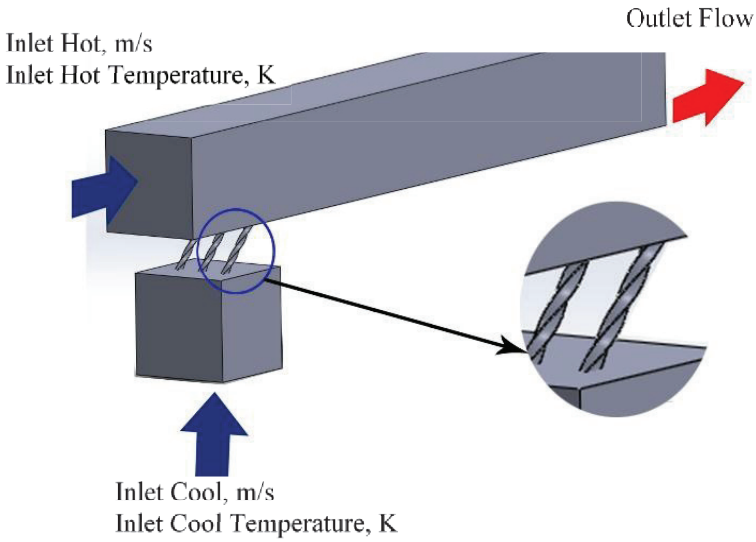

Fig.8 Boundary condition configuration.

3.2. Governing equations

The governing mathematical expression of the flow problem in the Cartesian coordinates system were derived from the following equations

Conservation of mass :

$$\nabla.\rho\vec{V} = 0 \quad (1)$$

Momentum equation:

$$\nabla.\left(\rho\vec{V}\,\vec{V}\right) = -\nabla P + \nabla.\left(\mu\nabla^2\vec{V}\right) \quad (2)$$

Energy equation:

$$\nabla.\left(\rho\,\vec{V}\,C_p\,T\right) = \nabla.\left(K\,\nabla T\right) \quad (3)$$

Results and Discussion of Heat Transfer

3.3. The Transient Heat Transfer Theory:

The transient heat flow over a flat plate maintained at an initial even temperature Ti, at time t > 0 is depicted in Fig. 9. The condition of the convective boundary was applied on the plate with the assumption that the conduction of heat ~~is~~ was mainly in x-direction. The energy balance on the plate was calculated using the following expression:

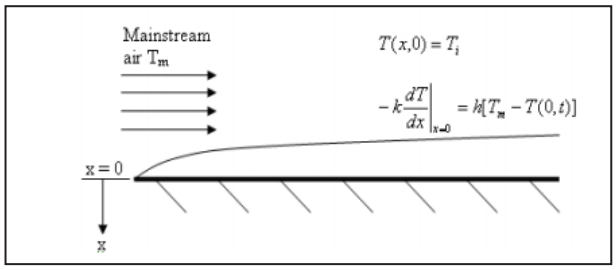

Fig. 9 Flow over a flat plate.

The 1-D transient conduction equation is expressed as:

$$\frac{\partial^2 \mathrm{T}}{\partial \mathrm{x}^2} = \frac{1}{\alpha}\frac{\partial \mathrm{T}}{\partial \mathrm{t}} \quad (5)$$

The boundary conditions (BC) was obtained from the following expression;

At x=0, $$-\mathrm{k}\frac{\partial \mathrm{T}}{\partial \mathrm{x}}\Big|_{\mathrm{x}=0} = \mathrm{h}\left[\mathrm{T_m} - \mathrm{T_{(0,t)}}\right]$$

The initial condition (IC) was derived from the expression below

At t=0, T=Ti

From Equation (5), one more BC is required in order to derive a solution since Eq. (5) is a partial differential equation of the 2nd order, where

Ti= Initial temperature of the test surface
Tw= the prescribed wall temperature
Tm= Mainstream temperature
α= Thermal diffusivity of test surface
k = Thermal conductivity of test surface
t = Time when the IR image was taken after the test was initiated.
h = Heat transfer coefficient

The convective boundary surface and the non-dimensional temperature of Incropera et. al. [21] was employed as shown in the expression below:

$$\frac{T_w - T_i}{T_m - T_i} = 1 - \left[\exp\left(\frac{h^2 \alpha t}{k^2}\right)\right] \operatorname{erfc}\left[\frac{h\sqrt{\alpha t}}{k}\right] \quad (6)$$

Locally mixed two streams were employed to evaluate the film temperature. For the purpose of this investigation, heat flux into the surface was calculated using the expression shown below:

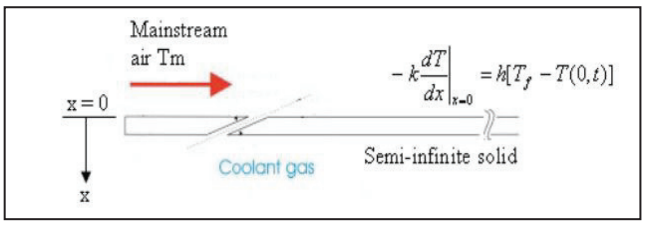

Fig. 10 Flow over a flat plate

In adiabatic surface, the temperature of the adiabatic wall the same with the film temperature, where the film temperature (T_f) and the heat transfer coefficient (h_f) were unknown variables.

Thus, the film cooling effectiveness (η), which is a non-dimensional temperature was employed to determine the unknown T_f given that T_m and T_c are known as depicted in Eq. (6):

$$\eta = \frac{T_f - T_m}{T_c - T_m}$$

Or

$$T_f = \eta(T_c - T_m) + T_m = \eta T_c + (1 - \eta) T_m \quad (7)$$

Such that values of the film cooling effectiveness falls within the range of 0 and 1 with regards to its lowest and highest values respectively.

By substituting T_m in Equation (7) with T_f in Equation (6), the equations for the two unknown variables, h and η were obtained as depicted in the following expression:

$$T_w - T_i = 1 - \left[exp\left(\frac{h^2 \alpha t}{k^2}\right)\right] erfc\left[\frac{h\sqrt{\alpha t}}{k}\right] \times [\eta T_c + (1 - \eta) T_m - T_i] \quad (8)$$

The results generated from the three test models were compared with experimental studies on standard smooth holes that were previously described [23]. The validation analysis is presented in Fig. 11 and comparison with previous studies [37, 39] are depicted in Fig. 12. Comparison between both the experimental as well as numerical data SST k- ω turbulence model are equally presented in Fig. 12. The results have demonstrated that the deviation was less than 2%, which falls within the acceptable range, and the numerical setup and the simulations were similarly acceptable.

The twisted angle was found to induce increase in the effectiveness, these forms causes:

• An increase in the angle of the vortices in jet flow.

• A decrease on the thermal stress exerted on the walls as a result of the difference in expansion with respect to the grill.

• Enables secondary movements of the fluid as a result of the alternating changes in the curves in order to maintain high pressure loss

• Increases the surface plates convection as.

From Fig. 13-15, it could be deduce that the optimum effectiveness was achieved at both the rectangular cross section as well as at twisted angle (360°) owing to the optimum vortices in the jet flow. These twisted film cooling holes produced a swirling within the blade of the turbine, with α angle to impingement with main stream.

It was found that increase in twisted angle (0°, 90°, 180°, 270° and 360°) induces corresponding increase in the effectiveness, while a decrease was recorded when the blowing ratio (BR) was increased owing to the fact that the jet flow becomes faster on surface of the blade turbine.

It was similarly found that the effectiveness of the rectangular hole shape increase when compared with the circular hole shape which ranges from 40 to 70.17% and from 40 to 65.523 % in the case of hexagonal cross section area.

The results were compared with the experimental data of straight fan shaped hole (standard smooth hole) by Sinha [37], and Pedersen, [39]. The conditions of previous experimental investigations have a BR of 1.5 and angle of secondary flow 35° as shown in Fig. 11. This figure has two regions, with each having specific symptoms. The first region of X/D_h range 1-5 exhibits a rapid decrease of cooling effectiveness and high cooling effectiveness value in the current experimental results comparison to the other pervious study [37, 39].

The second region exhibit a lesser decrease, but the cooling effectiveness value of current and literature reports were so closed. This behavior resulted owing to the different secondary coolant hole angle employed. The deviation between the current study and the other two studies were ±2.5% and ±3.5% respectively. This deviation is within the acceptable range, as it was mentioned in a previous related study Ghorab, 2009 [38] stated a maximum deviation ±10%.

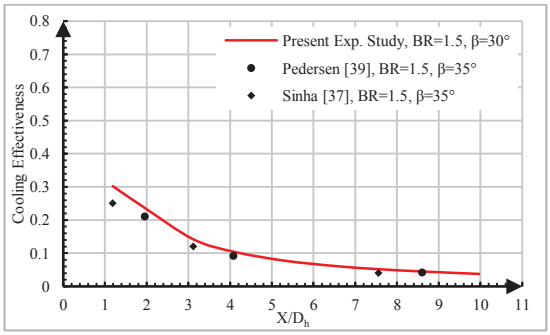

Fig. 11 Comparison between the conventional standard smooth hole [37] and [39] present experimental findings.

The reliability of the results is very important, because the validation helps to give an imagination for the obtained data whether the research going to wrong or right way. The lateral-averaged film cooling effectiveness was compared with a cylindrical smooth hole under similar test conditions, as depicted in Fig. 14. The BR was 1.5 while the inclination angle relative to the wall surface ~~is~~ was at 30°. Compared with studies conducted previously [40, 41], from X/D_h range of 1.0 – 10, except for a slight difference in values, the general tendency was consistent with the published findings of central averaged film cooling effectiveness as presented in Fig. 14. The deviation between the current study the two other two studies were ±2% and ±3% respectively.

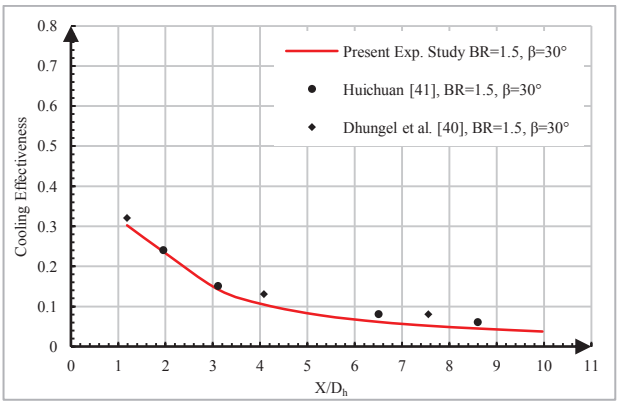

Fig. 12 Comparison between the conventional smooth hole [40, 41] and the present experimental findings

Fig. 13a shows that the secondary hole angle β = 30° has the optimal cooling effectiveness amongst all the arrangements at BR of 2.0, with β = 45° and β = 90° offering the least protection. The increased effectiveness values provided by the secondary cooling hole angle β = 30° continued at distances downstream greater than X/D_h 11.0.

It is imperative to note that the coverage values of all the holes are different when looking at this data. On the other hand, the coverage for β = 90° was 22% and 40% for β = 30°. This implies that the highest value of β = 30° which was at the exit of the holes should be towards η = 0.4, while it should only be 0.22 for β = 90°. The implications of this is discussed later in this section. Hence, only the general trends were discussed, in the context of BR parameters as outlined in the literature

At BR of 1.5, as presented in Fig.15b, hole angles β = 30°, β = 45° and β = 90° started lifting off. This is seen in the cooling effectiveness of the curves which were found to be at low X/D_h, and the subsequent upsurge and sustenance of the cooling effectiveness value of 0.45 at hole angles β = 30°, also flattens out, while hole angles β = 45° and hole angles β=90° show very similar values of η at more than X/D_h =10 as in BR=1.5. However, the performance of these three hole angles β=30°, β=45° and β=90°improves for values when compared to BR=2.0.

Fig. 13c presents the BR of 1.0. The result shows that the secondary hole angle β=30° offers the highest cooling effectiveness (η =0.48) of all the configurations at blowing ratio 2.0 and 1.5 with β=45° a3nd β=90° offering the least protection. The increased effectiveness values provided by the wider hole angle β=30° continue at distances downstream greater than X/D_h 10.

Fig. 13d presents the BR of a film cooling jet via a rectangular twisted hole of 0.5 improved the effectiveness of the film cooling. The findings offered the highest cooling effectiveness (η = 0.51) of all the configurations at BR 2.0, 1.5 and 1.0 with β = 45° and β = 90° offering the least protection. The improvement in film cooling effectiveness was as a result of the interactions between the swirling film jet and the mainstream. The swirling motion was noted to have destroyed the kidney vortex structure and subsequently made the film-cooling air adhere to the wall.

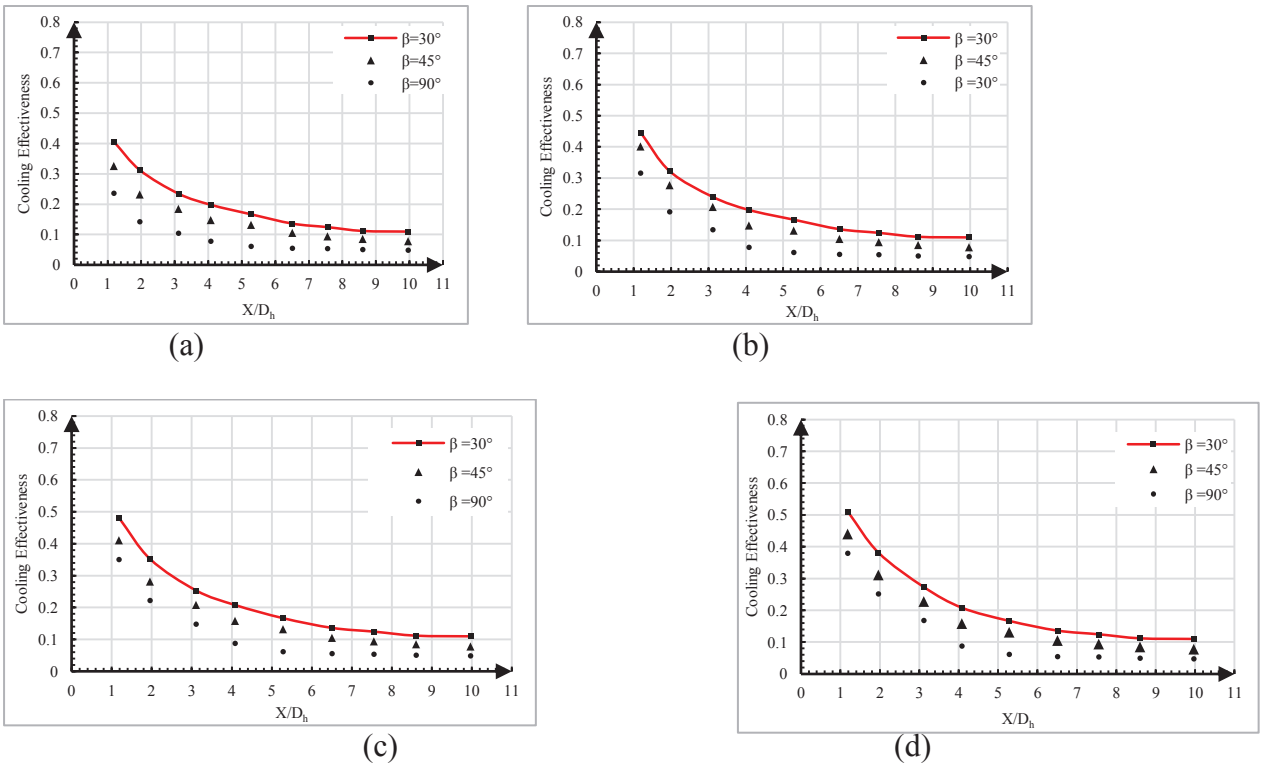

Fig. 13 Effectiveness against stream wise location at BR equal to ((a) BR= 2.0 (b) BR=1.5 (c) BR=1.0 (d) BR=0.5)

Fig. 14 depicts the local averaged film cooling effectiveness performances for the rectangular twisted hole for diverse downstream locations and at varying BRs of 0.5, 1.0, 1.5 and 2.0. The results demonstrated that at X/D_h of 1.2, the higher value of the effectiveness of the film cooling performance generated by the rectangular twisted hole was superlative compared to the standard smooth hole. The difference in film cooling performance between the two film hole arrangements indicated an increase more with decreasing BRs, as presented in figure.

The downstream film cooling effectiveness decreased along the streamwise direction for both configurations until reach X/D_h 11.0, owing to a decline in the momentum of the secondary flow. The averaged film cooling effectiveness performance of the rectangular twisted hole was still higher compared to the one generated by the circular hole at whole range of X/D_h from 1.2-11.0, as depicted in Fig. 16.

At a high BR of 2.0, the circular film hole provided a lateral film cooling performance near zero, as shown in Figure 5.8d.

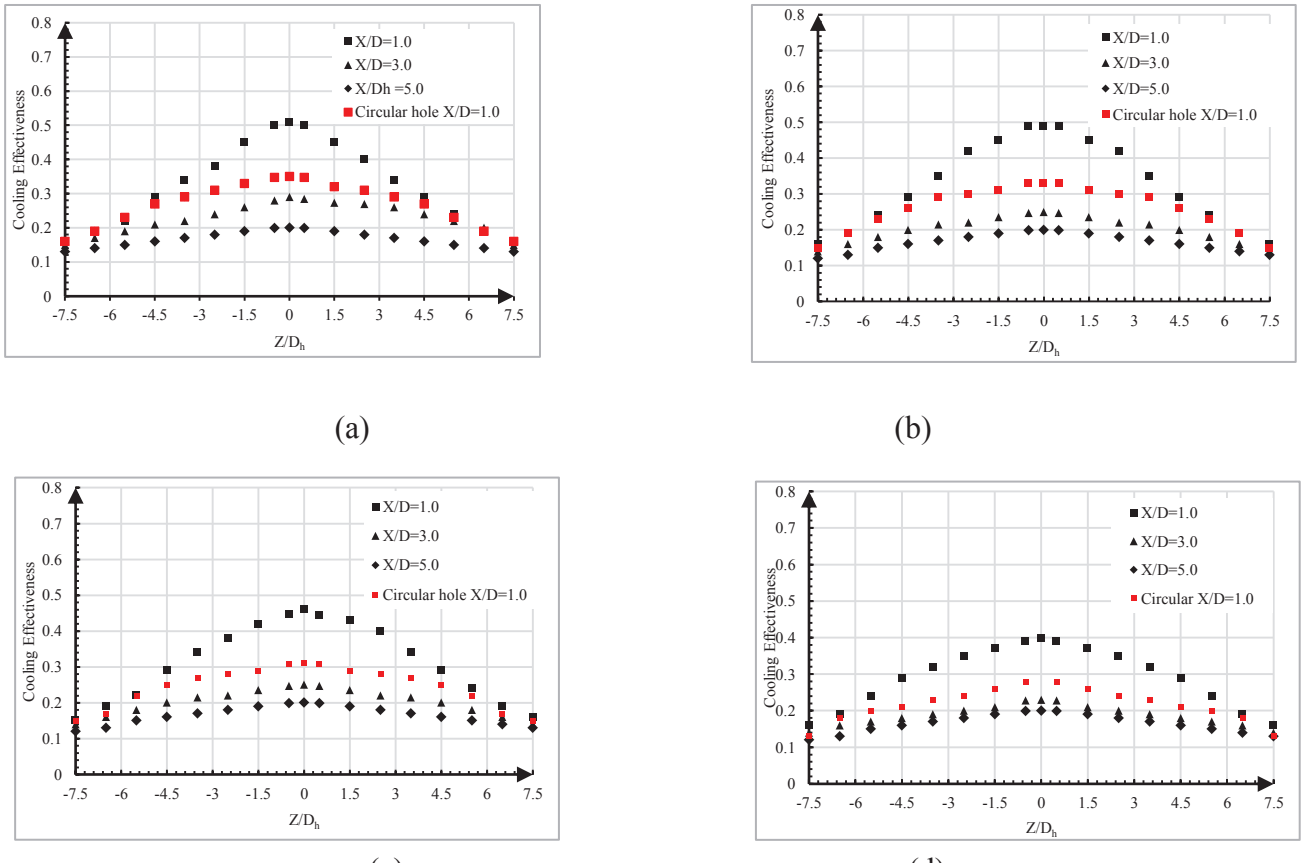

Fig. 14 Spanwise film cooling effectiveness of the twisted hole at diverse BRs (a) BR = 0.5 (b) BR = 1.0 (c) BR = 1.5 (d) BR = 2.0

Fig. 15.a depict the heat transfer ratio with twisted angle 360° highest point at X/D_h about ~ 2.0 near the injection hole. At lower BR, the twisted film cooling holes produce variations in the magnitude of the thermal transfer ratio. However, it provides a lower value downstream. . The result shows offers the optimal heat transfer ratio (h_f / h_0 =1.8) of all the other BR curves at 1.0, 1.5 and 2.0. The observed improvement emerged from the interactions between the swirling film jet, the mainstream as well as the swirling motion.

Fig. 15b shows the heat transfer ratio for the smooth rectangular shape hole highest point at X/D_h which was about ~ 2.0, corresponding to the highest values in heat transfer ratio (h_f / h_0 =1.5). The

proposed scheme produces a value of the centerline heat transfer coefficient ratio higher than unity near the trailing edge of the film holes. This was as a result of the high velocity in the boundary layer with three dimensional flow structures, near the film hole. Along the streamwise direction, the velocity decreases and gradually the flow become mainly two dimensional flow structures.

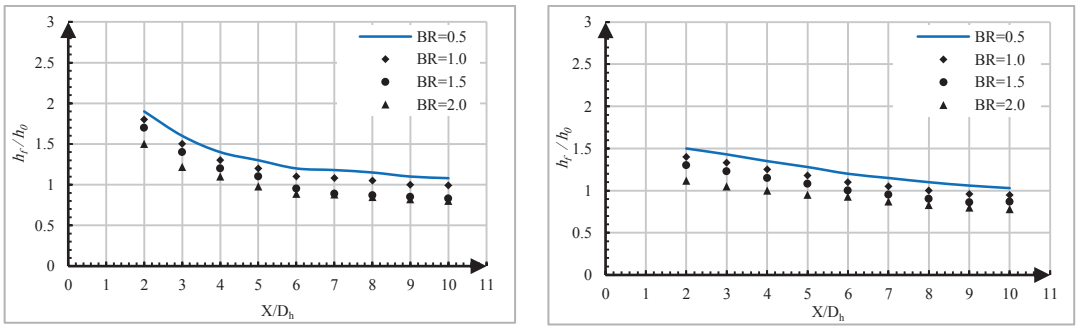

Figure 15 Heat transfer coefficient ratio vs. stream wise location
(a) α=360° (b) α=0°

4. Development of New Formula

Empirical correlations were commonly used to predict the Nusselt number and laterally averaged adiabatic cooling effectiveness. They are mathematical formulations of different levels of complexity derived from experimental results and may cover ranges of flow as well as geometrical parameters. When selecting a correlation model, two important topics should be considered, one related to the limitations of the model and the other concerning the predictability of the model.

$$Nu = f(Br, Pr, \alpha, \beta, n)$$

The computer package (STATISTICA) was used to make analysis for the equation through a non- linear regression analysis.

$$Nu = C_1(Br)^{C_2}(Pr)^{C_3}(\alpha)^{C_4}(\beta)^{C_5}(n)^{C_6}$$

C_1= 0.0045, C_2= -0.754, C_3= 0.513, C_4= 0.179, C_5= 0.847 and C_6=0.35

R^2 = 0.95

So, the equation becomes:

$$Nu = 0.0045\ (Br)^{-0.754}(Pr)^{0.513}(\alpha)^{0.179}(\beta)^{0.847}(n)^{0.35} \quad (9)$$

The coefficient of determination (R^2) for this formula was (0.95).
Another data is used to test the equation. A statistical comparison of equations is used to show the predicted convergence to observed records. The value of R^2 = 0.931 were observed to be in good agreement for all data as shown in Fig. 24.

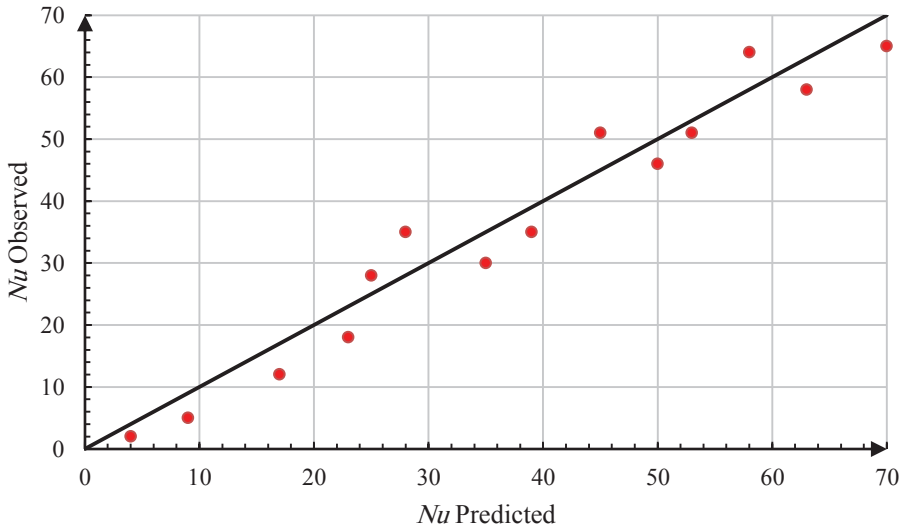

Fig. 16 Comparison of equation (9) with experimental data

The Nu correlation was generated for the data obtained from the experimental results by using Buckingham pi theorem. The correlation was compared with the findings of the experimental investigations in order to validate the ability of the correlation to predict the Nu and the error was found within ±9.0 %.

5. Conclusions

In this study, a three case spirally corrugated film cooling holes (one, two and three holes) were experimentally and numerically evaluated to determine the effects of new twisted film cooling hole angle (α) and angle of hole (β) on thermal efficiency and/or performance. The findings of this study revealed that the adopted geometry of film cooling hole with smooth spiral corrugations can significantly improve effectiveness, ranging from 2.2–3.4 times those of the smooth film cooling holes with significant increase in the overall heat transfer coefficient ranging from 1.5–2.7 times those from smooth film cooling holes. The best thermal performance at twisted film cooling angle (α) equal to 360° and angle of hole (β) equal to 30° at blowing ratio equal to 0.5. Based on the data obtained in this study, it was concluded that the most important factor in generating higher heat transfer coefficient as well as enhanced effectiveness– lies in adopting and modified geometry of film cooling holes with smooth spirally corrugation profile which has to be optimized for greater efficiency.

Nomenclature

Symbol	Quantity	Units
Br	blowing ratio ($\rho_j u_j/\rho_m u_m$)	-
C_p	specific heat	W/kg.k
D_h	hydraulic diameter of film hole (m)	m
d_h	hydraulic diameter of the main duct	m
DR	density ratio (ρ_j/ρ_m)	-
h	heat transfer coefficient	W/m^2. K
K	thermal conductivity of plate	W/m K
L	length of film hole	m

Nu	Nusselt number	-
p	film hole pitch	m
q	Heat transfer flux	W/m^2
Re	Reynolds number	-
T	temperature	K
t	time	s
T_w	average wall temperature	K
U_m	normal main stream velocity in x-direction	m/s
x, y, z	coordinates	
ά	thermal diffusivity	m^2/s
η	local film cooling effectiveness	-
β	Angle of holes	°
α	Angle of twisted holes	°

References

[1] Z.S. Kareem, M.N., Mohd Jaafar, T.M., Lazima, A., F. Abdulwahid, Passive heat transfer enhancement review in corrugation, Experimental Thermal and Fluid Science. (68)(2015) 22-38.

[2] A. F. Abdulwahid, , T. M. Lazim, A. Saat, Z. S. Kareem, Investigation of Effect Holes Twisted angle and Compound Angle of Holes on Film Cooling Effectiveness. International Review of Automatic Control. 8(3) (2015) 244-250.

[3] D. G. Bogard, Airfoil Film Cooling. The Gas Turbine Handbook, National Energy Technology Laboratory, Department of Energy, Morgantown, WV, Sect. (2006) 4.2.2.1.

[4] J. D. Heidmann, A Numerical Study of Anti-Vortex Film Cooling Designs at High Blowing Ratio, NASA Center for Aerospace Information, Glenn Research Center Cleveland, Ohio. (2008) 44135.

[5] S. Ramesh, D. G. Ramirez, S. V. Ekkad, M. A. Alvin, Analysis of film cooling performance of advanced tripod hole geometries with and without manufacturing features, International Journal of Heat and Mass Transfer 94 (2016) 9–19.

[6] Goldstein, R. J. Film Cooling. Adv. Heat Transf. (7) (1971) 321–379.

[7] Bogard, D. G., Thole, K. A. Gas Turbine Film Cooling. J. Propul. Power. (2006) 22: 249–270.

[8] V. L. Eriksen, R. J. Goldstein, Heat Transfer and Film Cooling Following Injection Through Inclined Circular Tubes. ASME J. Heat Transf. (1974)239–245.

[9] T. Elnady, I. Hassan, L. Kadem, T. Lucas, Cooling effectiveness of shaped film holes for leading edge, Experimental Thermal and Fluid Science 44 (2013) 649–661.

[10] R. J. Goldstein, E. R. G. Eckert, Effect of Hole Geometry and Density on Three-Dimensional Film Cooling. Int. J. Heat Mass Tran. (17) (1994) 595–607.

[11] J. Pu, J. Wang, S. Ma, X. Wu , An experimental investigation of geometric effect of upstream converging slot hole on end wall film cooling and secondary vortex characteristics. Experimental Thermal and Fluid Science. (69) (2015) 58–72.

[12] K. Takeishi, S. Aoki, Contribution of Heat Transfer to Turbine Blades and Vanes for High Temperature Industrial Gas Turbines: Part 1, Film Cooling. Ann. N. Y. Acad. Sci. (934) (2001) 305–312.

[13] Y. Yu, C. H. Yen, T. I. Shin, M. K. Chyu, Film Cooling Effectiveness and Heat Transfer Coefficient Distribution around Diffusion Shaped Holes. ASME J. Heat Transf. (124) (2000) 820–827.
[14] R. S. Bunker, A Review of Shaped Hole Turbine Film-Cooling Technology. ASME J. Heat Transf. (127) (2005) 441–453.
[15] L. Haiyong, L. Cunliang, W. Wenming, Numerical investigation on the flow structures in a narrow confined channel with staggered jet array arrangement, Chinese Journal of Aeronautics, (2015), 28(6): 1616–1628.
[16] Y. Zhang, X. Yuan, P. Ligrani, Film cooling effectiveness distribution on first-stage vane endwall with and without leading-edge fillets, International Journal of Heat and Mass Transfer (66) (2013) 642–654.
[17] A. F. Abdulwahid, T. M. Lazim, A. Saat, Z. S. Kareem, Experimental Thermal Field Measurements of Film Cooling with Twisted Holes, International Review of Aerospace Engineering. 8(3) (2015) 86-94.
[18] S. H. Han, D. Chang, J. S. Kim, Experimental investigation of highly pressurized hydrogen release through a small hole, international journal of hydrogen energy. (39) (2014) 9552-9561
[19] H. P. Kissel, B. Weigand, J. Wolfersdort, von Neumann, S. O., and Ungewickell، A. An Experimental and Numerical Investigation of the Effect of Cooling Channel Cross flow on Film Cooling Performance. ASME Paper GT-2007-27102. (2007).
[20] Y. Kuya, C. Nuntadusit, H. Ishida, K. Momose, H. Kimoto, An Application of Swirling Jet to Film Cooling. Proc., JSME Thermal Engineering Conference, Sendai, No. 04-28. (2004).
[21] A. F. Abdulwahid, T. M. Lazim, A. Saat, Z. S. Kareem, Investigation of Effect Holes Twisted Angle and Compound Angle of Holes on Film Cooling Effectiveness, International Review of Automatic Control. 8(3) (2015) 244-250.
[22] Takeishi, K., Kitamura, T., Komiyama, M., Oda, Y., Mori, S. Study on the Thermal and Flow Fields of Shaped Film Cooling Holes. Int. Symp. On Heat Transfer in Gas Turbine Systems, Antalya, Turkey. 2009.
[23] Incropera, F. P., DeWitt, D. P. Introduction to Heat Transfer, New York: John Wiley & Sons. 2002.
[24] Kareem, Z.S., Mohd Jaafar, M.N., Lazima, T.M., Abdullahb, S., Abdulwahid, A. F. Passive heat transfer enhancement review in corrugation. Experimental Thermal and Fluid Science. 2015; 68: 22-38.
[25] D. H. Leedom, S. Acharya, Large Eddy Simulations of Film Cooling Flow Fields from Cylindrical and Shaped Holes. In Proceedings of ASME Turbo Expo 2008. Berlin, Germany. (2008).
[26] S.J. Kline, F.A. McClintock, Describing uncertainties in single-sample experiments. Mechanical Engineering. (75) (1953) 3-8.
[27] S.P. Veluri, Code verification and numerical accuracy assessment for finite volume CFD code. Ph. D. Thesis. Virginia Polytechnic Institute and State University. USA. (2010).
[28] R. Zhang, Y. Zhang, K.P. Lam, D.H. Archer, A Prototype mesh generation tool for CFD simulations in architecture domain. Building and Environment. (45) (2010) 2253-2262.
[29] A. Skoglund, Preservation of wakes in coarse grid CFD. MSc Thesis. Chalmers University of Technology, Sweden. 2008.
[30] M.M. Noor, A. P. Wandel, T. Yusaf, Detail guide for CFD on the simulation of biogas combustion in bluff-body mild burner. ICMER Conference, Kuantan, Malaysia. (2013).
[31] Q. Xiong, S. Aramideh, A. Passalacqua, S. Kong, Characterizing effects of the shape of screw conveyors in gas–solid fluidized beds using advanced numerical models. ASME Journal of Heat Transfer. (137) (2015) 061008.
[32] H. Han, B. Li, B. Yu, Y. He, F. Li, Numerical study of flow and heat transfer characteristics in outward convex corrugated tubes. International Journal of Heat and Mass Transfer. (55) (2012) 7782–7802.

[33] P. J. Roache, Perspective: A Method for uniform reporting of grid refinement studies. Journal of Fluids Engineering. (116) (1994) 405-41.
[34] L.F. Richardson, J.A. Gaunt, The deferred approach to the limit. Part I. Single Lattice. Part II. Interpenetrating Lattices. Philosophical Transactions of the Royal Society of London. (226) (1927) 299-361.
[35] D.C. Wilcox, Turbulence Modeling for CFD, third ed. Pratyush Peddireddi, California. (2006).
[36] Kohli, A., Bogard, D.G. Adiabatic Effectiveness, Thermal Fields, and Velocity Fields for Film Cooling with Large Angle Injection. ASME J. Turbomachinery. (119) (1997) 352-358.
[37] A.K. Sinha, D.G. Bogard, M.E. Crawford, Film Cooling Effectiveness Downstream of a Single Row of Holes with Variable Density Ratio, ASME J. Turbomachinery. (113) (1991) 442–449.
[38] Ghorab, M. G., Experimental investigation of advanced film cooling schemes for a gas turbine blade. Ph. D. Thesis, Concordia University, (2009).
[39] D. R. Pedersen, E. R. G. Eckert, R. J. Goldstein, Film Cooling with Large Density Difference between the Mainstream and the Secondary Fluid Measured by the Heat-Mass Transfer Analogy, ASME J. Heat Transfer. (99) (1977) 620–627.
[40] A. Dhungel, Y. Lu, W. Phillips, S. V. Ekkad, J. Heidmann, Film cooling from a row of holes supplemented with anti-vortex holes. Journal of Turbomachinery. 131(2) (2009) 021007.
[41] H. W. Huichuan, C. Y. Li, , Rong, C., Ding, S., Effects of side hole position and blowing ratio on sister hole film cooling performance in a flat plate. Applied Thermal Engineering. (93) (2016) 718–730.